

Original articles

Regular and chaotic dynamics in a 2D discontinuous financial market model with heterogeneous traders

Iryna Sushko^{a,*}, Fabio Tramontana^b^a Institute of Mathematics, NAS of Ukraine, and Kyiv School of Economics, Kyiv, Ukraine^b Department of Economics, Society and Politics, University of Urbino, Italy

ARTICLE INFO

Keywords:

Two-dimensional discontinuous map
 Bifurcation structure of the parameter space
 Border-collision bifurcations
 Regular and chaotic attractors
 Degenerate bifurcations
 Financial market model with heterogeneous traders

ABSTRACT

We develop a financial market model where three types of traders operate simultaneously: fundamentalists and chartists of two types, namely, trend followers and contrarians. The dynamics of this model is described by a two-dimensional discontinuous map defined by two linear functions, where one acts in the partition between two (parallel) discontinuity lines and the other one acts outside this partition. Our analysis shows that despite the linearity of the map components, its dynamics can be quite complex, with various, possibly coexisting attracting cycles and chaotic attractors. As a first step towards the understanding how the overall bifurcation structure observed in the parameter space of the map is organized, we obtain analytically the boundaries of periodicity regions related to the simplest attracting period- n cycles, $n \geq 3$, with one point in the middle partition and $n - 1$ points outside it. These boundaries can be related to border-collision bifurcations (when a point of the cycle collides with a discontinuity line) as well as to degenerate bifurcations (associated with eigenvalues on the unit circle). We show also some elements of period-adding and period-incrementing bifurcation structures for which the cycles mentioned above are basic. From an economic point of view, our study confirms that a fairly simple financial market model with heterogeneous agents is able to produce complicated boom-bust dynamics typical of real financial markets.

1. Introduction

A time series of asset prices which are at the same time both bounded and hardly predictable can be obtained by building dynamic models with regime switching, that is described by piecewise-defined dynamic equations, and not necessarily by introducing some nonlinearities into the equations. The pioneering contribution to this field is the work of Huang and Day [11].¹ In particular, they consider traders whose reaction to the misalignment (i.e. difference between the current price and its fundamental value) depends upon the crossing or not of a certain price threshold. Their model is piecewise-linear (with five branches) and allows us to obtain chaotic dynamics of the asset price. This model has been more recently extended in several papers by Tramontana et al. [27,28,29], where asymmetry in the reaction of the traders is introduced. When the asset is overvalued or undervalued the reactions can be different, and this produces interesting dynamics also in the case of two or three branches. On the other hand, [12,13] replicate the so-called sudden, disturbing and smooth crisis by increasing the number of branches of the piecewise-linear model. All these models

* Corresponding author.

E-mail addresses: sushko@imath.kiev.ua (I. Sushko), fabio.tramontana@uniurb.it (F. Tramontana).

¹ While [6] is more popular and is a seminal paper for the literature on financial markets populated with heterogeneous agents, [11] is quite important because in this work they obtain similar results of their former work without introducing nonlinearities in the picture and replacing them with piecewise-linear behavioral rules.

<https://doi.org/10.1016/j.matcom.2024.01.021>

Received 2 December 2023; Received in revised form 20 January 2024; Accepted 24 January 2024

Available online 29 January 2024

0378-4754/© 2024 International Association for Mathematics and Computers in Simulation (IMACS). Published by Elsevier B.V. All rights reserved.

share the feature of being one-dimensional (1D for short). In the last years, several authors have started building financial market models with heterogeneous traders, leading to two-dimensional (2D for short) systems. With two dimensions, in fact, it is possible to introduce into the picture also other kinds of traders like trend-followers and contrarians. Among papers associated with this direction of the research, [1,8–10,16] deserve to be mentioned for their success in replicating several important stylized facts of the financial markets, such as fat tails, linear and nonlinear dependence of returns in time, volatility clustering (see, e.g., [5,14,15]).

A financial market model proposed in the present paper deals with three types of traders which are fundamentalists and chartists of two types — trend followers and contrarians. The dynamics of this model is defined by a 2D piecewise-linear map F with two parallel discontinuity lines dividing the state space into three partitions. It is worth mentioning that the dynamics of a financial market model considered in [10] is defined by a map belonging to the same class. However, in [10], the maps acting in three partitions have the same Jacobian matrix and differ only by the offsets, while in our case, one map acts in the middle partition and the other one outside it, and these two maps have different Jacobian matrices and offsets. Moreover, depending on the parameters, map F can have various types of invertibility, with zones having 0, 1 or 2 preimages, while the map studied in [10] has only zones with 0 or 1 preimages. Recall that in a generic 2D nonlinear map, the zones associated with the different number of preimages are separated by the critical lines (see [18] which in our case are images of the discontinuity lines. Recall also that the invertibility of a map is an important characteristic: for example, an attractor of a 2D invertible map can have points neither in zone with 0 preimages, nor in any its image.

The properties mentioned above as well as other properties of map F , lead to a rather complex bifurcation structure of the parameter space, with periodicity regions, often overlapping, associated with various attracting cycles, and regions related to chaotic attractors of different kinds. In this structure, due to the linearity of the components of map F , the boundaries of a periodicity region can be related either to a border collision bifurcation² occurring when some periodic point collides with a discontinuity line, or to a degenerate bifurcation (see [25]) related to an eigenvalue $+1$, -1 or to a pair of complex-conjugate eigenvalues on the unit circle. The present paper can be seen as a first step towards the understanding of the organizing principles of this structure. Studies related to various bifurcation structures in 2D discontinuous maps can also be found in [1,2,4,17,21,23,26], etc.

This paper is organized as follows. In the next section, we describe some basic steps in the construction of the financial market model with three kinds of speculators (fundamentalists, trend-followers and contrarians), leading to a 2D piecewise linear discontinuous map F . Then, in Section 3 we present the simplest properties of F which is defined by two linear maps: map F_M acts in the middle partition bounded by two parallel discontinuity lines, and map F_E acts outside this partition. In particular, we obtain the stability conditions of the actual and virtual fixed points of map F , describe center bifurcation of the actual fixed point, examine different kinds of invertibility of F depending on the parameters. A few examples of the bifurcation structures obtained numerically are presented in Section 4, in particular, elements of period-adding³ and period-incrementing⁴ bifurcation structures are illustrated by 1D bifurcation diagrams. Basic cycles for these structures can be represented by the symbolic sequences ME^{n-1} for $n \geq 3$, where the symbol M corresponds to a periodic point in the middle partition and the symbol E to periodic points which are external to this partition. In Section 5 we explain how to analytically obtain the existence and stability boundaries of the periodicity regions associated with attracting cycles ME^{n-1} . As already mentioned, these boundaries can be related either to border-collision bifurcations (associated with a collision of some point of a cycle ME^{n-1} with a discontinuity line) or to degenerate bifurcations. Section 6 concludes.

2. Description of the model

We model a financial market of one asset with a market maker and three kinds of speculators. The market maker adjusts the price (P) of the asset with respect to the total excess demand (D) of traders by using the following linear trading rule:

$$P_{t+1} = P_t + \alpha D_t, \tag{1}$$

where $\alpha > 0$ is a price adjustment parameter.

Concerning speculators, we consider a group of fundamentalists and two groups of chartists.

Fundamentalists buy the asset when it is underpriced (that is, the price is lower than the fundamental value P^*) and sell it when it is overpriced (that is, the price is higher than the fundamental value). Their excess demand is:

$$D^f = f_1 + f_2(P^* - P_t) \tag{2}$$

where $f_2 > 0$ is their reactivity with respect to the misalignment, while f_1 captures some kind of optimism/pessimism when the price is equal to its fundamental value (see [27,29]).

We consider two groups of chartists. They both observe the most recent price trend ($P_t - P_{t-1}$) but while a group bets on the persistence of the trend (*trend-followers*), the second one does exactly the opposite, betting on a trend reversal (*contrarians*).

² This term is introduced in [19], see also [20]. Border collision bifurcations, which are characteristic for nonsmooth maps, are nowadays actively studied both from theoretical and applied points of view (see, e.g. [3,7,22,30], to cite a few).

³ Recall that in a period-adding bifurcation structure periodicity regions related to attracting cycles are ordered according to Farey summation rule applied to rotation numbers of the related cycles. In this way, between periodicity regions associated with rotation numbers m_1/n_1 and m_2/n_2 with $|m_1n_2 - m_2n_1| = 1$ (so-called Farey neighbors) there exists a periodicity region related to cycles with rotation number $(m_1 + m_2)/(n_1 + n_2)$ (see [3] for details).

⁴ Period-incrementing structure is formed by periodicity regions ordered according to period of the cycles, which is increasing by $k \geq 1$ (incrementing step), where each two neighbor periodicity regions are partially overlapping.

Moreover, following [16], we assume that their reactivity depends upon the absolute value of the trend. When it is larger than a certain threshold⁵ (k) they react more strongly to the market signal.

The excess demand of trend-followers (or extrapolators) is:

$$D_t^f = \begin{cases} a_1 + b_1(P_t - P_{t-1}) & \text{if } |P_t - P_{t-1}| \leq k \\ a_2 + b_2(P_t - P_{t-1}) & \text{if } |P_t - P_{t-1}| > k \end{cases} \tag{3}$$

with reactivities $b_2 \geq b_1 \geq 0$ in order to characterize a more aggressive behavior when the trend is larger than the threshold. Parameters a_1 and a_2 capture optimism/pessimism when the trend is less or more accentuated, respectively.

The last excess demand we consider is the one of contrarians, which is the following:

$$D_t^c = \begin{cases} c_1 + d_1(P_{t-1} - P_t) & \text{if } |P_t - P_{t-1}| \leq k \\ c_2 + d_2(P_{t-1} - P_t) & \text{if } |P_t - P_{t-1}| > k \end{cases} \tag{4}$$

with reactivities $d_2 \geq d_1 \geq 0$ in order to characterize, similarly to the case of trend-followers, a more aggressive behavior when the trend is larger than the threshold. Parameters c_1 and c_2 capture optimism/pessimism when the trend is less or more accentuated, respectively.

The total excess demand is obtained by summing up the three excess demands:

$$D_t = D_t^f + D_t^e + D_t^c$$

and by replacing excess demands (2), (3) and (4) into the market maker Eq. (1) we get:

$$P_{t+1} = \begin{cases} P_t + \alpha [f_1 + f_2(P^* - P_t) + a_1 + b_1(P_t - P_{t-1}) + c_1 + d_1(P_{t-1} - P_t)] & \text{if } |P_t - P_{t-1}| \leq k, \\ P_t + \alpha [f_1 + f_2(P^* - P_t) + a_2 + b_2(P_t - P_{t-1}) + c_2 + d_2(P_{t-1} - P_t)] & \text{if } |P_t - P_{t-1}| > k, \end{cases} \tag{5}$$

which is a second order piecewise-defined difference equation regulating the dynamics of the price as a consequence of the trading strategies adopted by the three groups of traders.

By defining $x \equiv P - P^*$ as the deviation from the fundamental and the lagged variable $y_t = x_{t-1}$ we obtain the following map after some algebraic manipulation:

$$\begin{cases} x' = \begin{cases} \alpha (a_1 + c_1 + f_1 + f_2 P^*) + x (1 + ab_1 - ad_1 - \alpha f_2) + y\alpha (d_1 - b_1) & \text{if } |x - y| \leq k, \\ \alpha (a_2 + c_2 + f_1 + f_2 P^*) + x (1 + ab_2 - ad_2 - \alpha f_2) + y\alpha (d_2 - b_2) & \text{if } |x - y| > k, \end{cases} \\ y' = x \end{cases} \tag{6}$$

It is easy to see that in (6) we can set $\alpha = 1$ since all the parameters (except for k) can be redefined as $a_1 \equiv \alpha a_1$, $a_2 \equiv \alpha a_2$, etc. The parameters must satisfy the following conditions:

$$\begin{aligned} d_{1,2} > 0, \quad b_{1,2} > 0, \quad d_2 \geq d_1, \quad b_2 \geq b_1, \quad k > 0, \\ f_1 \in \mathbb{R}, \quad f_2 > 0, \quad a_{1,2} \in \mathbb{R}, \quad c_{1,2} \in \mathbb{R} \end{aligned} \tag{7}$$

3. Preliminaries

The map given in (6) is defined by two linear maps denoted F_M and F_E . Here index M refers to the middle partition

$$D_M = \{(x, y) : |x - y| \leq k\}$$

bounded by two discontinuity lines (also called critical lines of rank -1) denoted

$$C_{-1}^- = \{(x, y) : y = x - k\}, \quad C_{-1}^+ = \{(x, y) : y = x + k\}$$

and index E refers to the external region

$$D_E = \{(x, y) : |x - y| > k\}$$

which can be split in two partitions, $D_E = D_L \cup D_U$:

$$D_L = \{(x, y) : y < x - k\}, \quad D_U = \{(x, y) : y > x + k\}$$

It is convenient to change variables, $x := x - x^*$, $y := y - y^*$, where $x^* = y^* = (a_1 + c_1 + f_1 + P^* f_2) / f_2$, shifting the fixed point of the map defined in the middle partition to the origin. After this shift, map F can be defined as follows:

$$F : (x, y) \rightarrow F(x, y) = \begin{cases} F_M(x, y), & \text{if } (x, y) \in D_M \\ F_E(x, y), & \text{if } (x, y) \in D_E \end{cases} \tag{8}$$

where

$$F_M : \begin{pmatrix} x \\ y \end{pmatrix} \rightarrow \begin{pmatrix} x(b - k_1) + yk_1 \\ x \end{pmatrix}$$

⁵ For simplicity we assume the same threshold k for both contrarians and trend-followers. This prevents the creation of too many branches for the final map.

$$F_E : \begin{pmatrix} x \\ y \end{pmatrix} \rightarrow \begin{pmatrix} x(b - k_2) + yk_2 + d \\ x \end{pmatrix}$$

Here, for short, we introduced new aggregate parameters:

$$k_1 = d_1 - b_1, \quad k_2 = d_2 - b_2, \quad b = 1 - f_2, \quad d = (a_2 + c_2) - (a_1 + c_1)$$

Since $f_2 > 0$ (see (7)), it has to be $b < 1$, while parameters k_1, k_2, d and k can take any real value. Moreover, one could get rid of parameter d or k , e.g., introducing new variables $x := x/d, y := y/d, d \neq 0$, and a new parameter $h := k/d$. However, we prefer to keep both these parameters in our considerations. Basically, parameter k_1 (resp. k_2) can be interpreted as the excess of reactivity of trend-followers with respect to contrarians in the presence of a positive (resp. negative) trend. By contrast, the parameter d represents the difference between $(a_2 + c_2)$ (representing the optimism, if positive, or pessimism, if negative, of chartists, both trend-followers and contrarians, when the trend is more accentuated than the threshold k) and $(a_1 + c_1)$ (representing the optimism, if positive, or pessimism, if negative, of chartists when the trend is less accentuated than the threshold k). Below we suppose that $d > 0$ since for $d < 0$ map F has qualitatively similar dynamics (its invariant sets are symmetric with respect to the origin to those for $d > 0$).

Property 1. *The fixed point of F_M denoted $O(0, 0)$ is the unique actual fixed point of F , since the fixed point of map F_E , denoted $V(x_E^*, y_E^*)$, with*

$$x_E^* = y_E^* = \frac{d}{1 - b} \tag{9}$$

belongs to the middle partition D_M (namely, to the main diagonal), thus, it is always a virtual fixed point for F .

Property 2. *The fixed point O of map F is attracting iff $-1 < k_1 < (1 + b)/2$ (this range is non empty for $b > -3$).*

It is easy to check this property considering the Jacobian matrix J_M of F_M :

$$J_M = \begin{pmatrix} b - k_1 & k_1 \\ 1 & 0 \end{pmatrix} \tag{10}$$

Its characteristic polynomial $P(\lambda) = \lambda^2 - (b - k_1)\lambda - k_1$ has roots (eigenvalues) satisfying $|\lambda_{1,2}| < 1$ iff $\{\det J_M < 1, P(-1) > 0, P(1) > 0\}$ that corresponds to $\{k_1 > -1, k_1 < (1 + b)/2, b < 1\}$. Here $b < 1$ follows from (7), thus the stability conditions for O are $-1 < k_1 < (1 + b)/2$. Note that the eigenvalues $\lambda_{1,2} = (b - k_1 \pm \sqrt{(b - k_1)^2 + 4k_1})/2$ are complex-conjugate for $b - 2 - 2\sqrt{1 - b} < k_1 < b - 2 + 2\sqrt{1 - b}$.

Changing k_1 to k_2 in (10) we get the Jacobian matrix J_E of map F_E . Clearly, the stability conditions $-1 < k_2 < (1 + b)/2$ of the virtual fixed point V are also important for the dynamics of F since these conditions govern the behavior of the trajectories in region D_E .

Property 3. *For $k_1 = -1, -3 < b < 1$, the fixed point O of map F undergoes a center bifurcation ($\lambda_{1,2}$ are complex-conjugate and $|\lambda_{1,2}| = 1$). In this case, (a) if the rotation number of J_M is rational, say m/n (that holds for $b = 2 \cos(2\pi m/n) - 1$), then there exists an invariant polygon $P_{m/n}$ filled with n -cycles with rotation number m/n , bounded by the generating segments of the discontinuity lines C_{-1}^-, C_{-1}^+ and their images by F_M ; (b) if the rotation number of J_M is irrational, then there exists an invariant region \mathcal{E} filled with invariant ellipses any point of which is quasiperiodic, bounded by an ellipse with center at O which is tangent to C_{-1}^-, C_{-1}^+ and to all their images by F_M .*

Property 3 is illustrated in Fig. 1 : in (a) an invariant polygon $P_{1/8}$ (filled with 8-cycles with rotation number $1/8$) coexists with an attracting 7-cycle, and in (b) an invariant region \mathcal{E} (filled with quasiperiodic trajectories where each one is located on the related invariant ellipse) coexists with attracting 5- and 12-cycles. In both figures preimages of the invariant regions are shown in white. For details related to center bifurcations we refer to [24].

The critical lines, which are the images of the discontinuity lines C^\pm by F_M and F_E , are denoted, respectively, as $C^{M\pm} = F_M(C_{-1}^\pm)$ and $C^{E\pm} = F_E(C_{-1}^\pm)$:

$$\begin{aligned} C^{M-} : y &= (x + kk_1)/b, & C^{M+} : y &= (x - kk_1)/b \\ C^{E-} : y &= (x + kk_2 - d)/b, & C^{E+} : y &= (x - kk_2 - d)/b \end{aligned}$$

All these lines have the same slope $s = 1/b$ (positive for $b > 0$ and negative for $b < 0$). In this way, the region D_M bounded by the discontinuity lines C_{-1}^\pm is mapped by F_M and F_E in two strips, say, S^M and S^E , bounded by $C^{M\pm}$ and $C^{E\pm}$, respectively (see Fig. 2).

The invertibility of map F depends on the mutual location of the strips S^M and S^E . For example, if $S^M \cap S^E = \emptyset$ (as e.g., in Fig. 2(a)), then map F belongs to a class of maps with $Z_1-Z_2-Z_1-Z_0-Z_1$ type of invertibility,⁶ where $Z_0 = S^E$ (shown white in Fig. 2(a)), so that any point of S^E has no preimages. Map F has the same type of invertibility if S^E and S^M are partially overlapping (as in Fig. 2(d)), while if $S^M \subset S^E$ (as in Fig. 2(b)), then map F is of $Z_1-Z_0-Z_1-Z_0-Z_1$ type, that is, there are two strips with no preimages. This information is important: since points in Z_0 have no preimages, an invariant set of map F cannot have points in Z_0 , and if map F is invertible, then its invariant set cannot have point also in $F^i(Z_0)$ for any $i \geq 1$. In particular, if in such a case

⁶ Index i in Z_i indicates the number of preimages in zone Z_i .

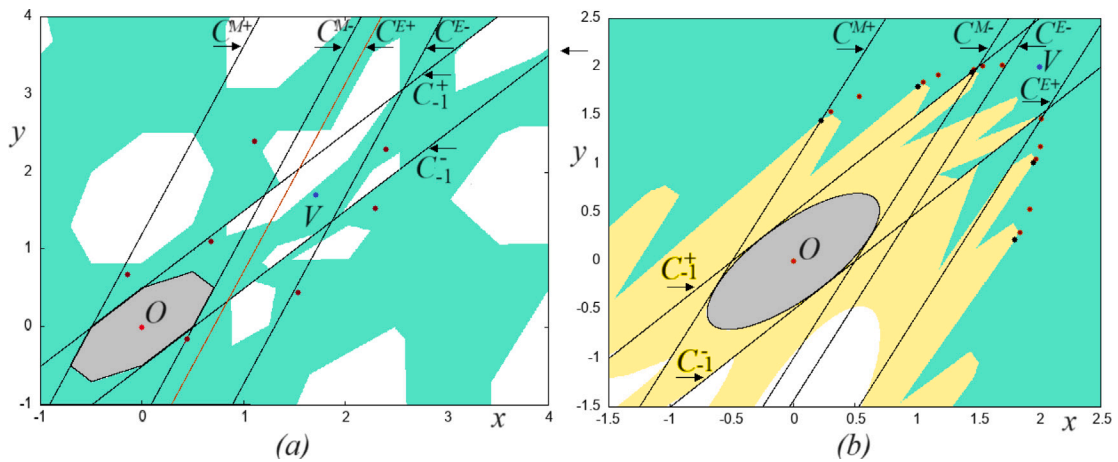


Fig. 1. Center bifurcation of the fixed point O : (a) an invariant polygon $P_{1/8}$ (shown gray with white preimages) filled with 8-cycles, coexists with an attracting 7-cycle (its basin is shown green); (b) an invariant region \mathcal{E} (shown gray with white preimages) filled with quasiperiodic trajectories, coexists with attracting 5- and 12-cycles (their basins are shown yellow and green, respectively). Here at $k_1 = -1$, $d = 1$, $k = 0.5$ and (a) $b = \sqrt{2} - 1$, $k_2 = -0.6$, (b) $b = 0.5$, $k_2 = 0.562$. (For interpretation of the references to color in this figure legend, the reader is referred to the web version of this article.)

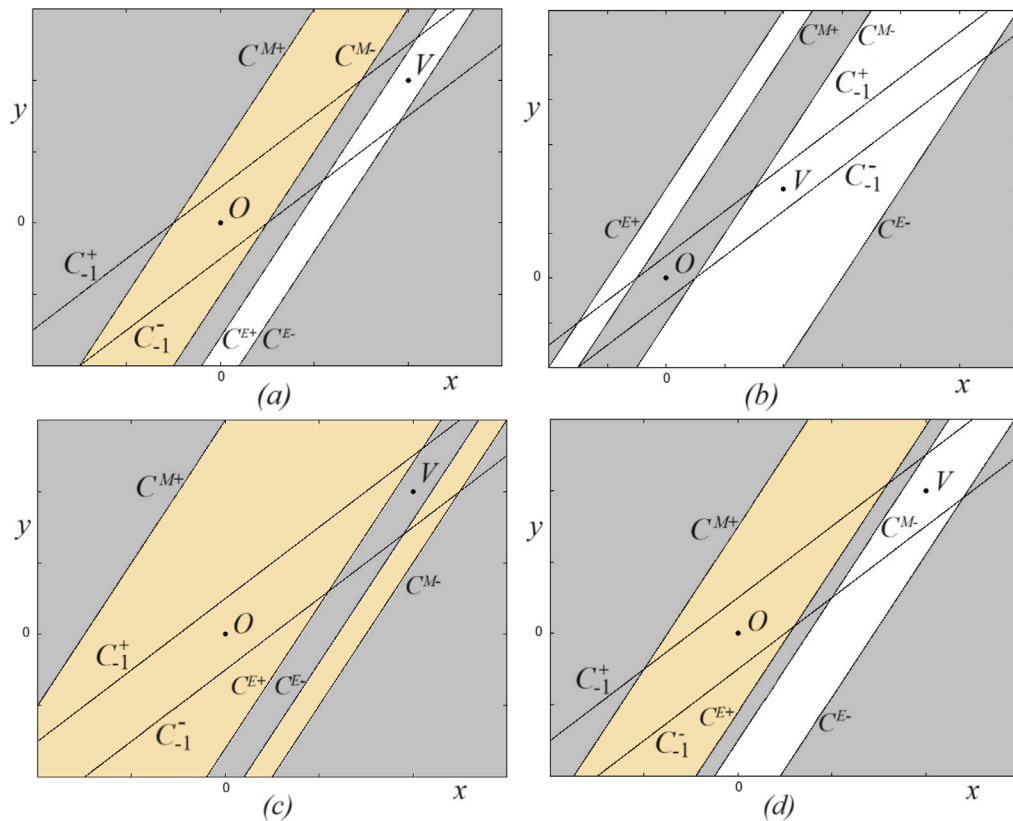


Fig. 2. Schematic representation of the images of region D_M (bounded by the discontinuity lines C_{-1}^- and C_{-1}^+): the strip $S^M = F^M(D_M)$ is bounded by C^{M+} and C^{M-} , and the strip $S^E = F^E(D_M)$ is bounded by C^{E+} and C^{E-} . Here the regions shown white, gray and yellow correspond to Z_0 , Z_1 and Z_2 zones, whose points have 0, 1 and 2 preimages, respectively. (a) $(k_1, k_2) \in R_I$, (b) $(k_1, k_2) \in R_{II}$, (c) $(k_1, k_2) \in R_{III}$, (d) $(k_1, k_2) \in R_{IV}$, where the regions R_I , R_{II} , R_{III} and R_{IV} are specified in Fig. 3. (For interpretation of the references to color in this figure legend, the reader is referred to the web version of this article.)

map F has an attractor, it must belong to a residual set $\Omega = \mathbb{R}^2 \setminus \cup_{i=0}^{\infty} F^i(Z_0)$ (as e.g., in Fig. 4(b)). Similar cases are described in [9,10].

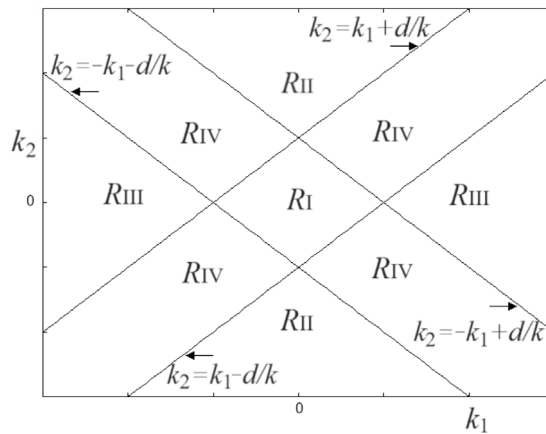


Fig. 3. Schematic representation of the partitioning of the (k_1, k_2) -parameter plane into regions related to invertibility of map F : it is of $Z_1-Z_2-Z_1-Z_0-Z_1$ type in R_I and in R_{IV} (see examples in Fig. 2(a) and Fig. 2(d), respectively), $Z_1-Z_0-Z_1-Z_0-Z_1$ type in R_{II} (see Fig. 2(b)), and $Z_1-Z_2-Z_1-Z_2-Z_1$ type in R_{III} (Fig. 2(c)).

The invertibility of F can be represented using the partitioning of the (k_1, k_2) -parameter plane by the straight lines of equations $k_2 = k_1 + d/k$, $k_2 = -k_1 + d/k$, $k_2 = -k_1 - d/k$ and $k_2 = k_1 - d/k$ (related to overlapping critical lines, $C^{E-} = C^{M-}$, $C^{E+} = C^{M+}$, $C^{E+} = C^{M-}$ and $C^{E+} = C^{M+}$, respectively), as schematically illustrated in Fig. 3 and summarized in

Property 4. *Invertibility of map F is of*

- $Z_1-Z_2-Z_1-Z_0-Z_1$ type, with $S^M \cap S^E = \emptyset$ (as e.g., in Fig. 2(a)) for $(k_1, k_2) \in R_I$, or with partially overlapping S^M and S^E (as e.g., in Fig. 2(d)) for $(k_1, k_2) \in R_{IV}$;
- $Z_1-Z_0-Z_1-Z_0-Z_1$ type, with $S^M \subset S^E$ (as e.g., in Fig. 2(b)) for $(k_1, k_2) \in R_{II}$;
- $Z_1-Z_2-Z_1-Z_2-Z_1$ type, with $S^E \subset S^M$ (as e.g., in Fig. 2(c)) for $(k_1, k_2) \in R_{III}$.

To illustrate Property 4 we present examples of various chaotic attractors of map F for $(k_1, k_2) \in R_I$ in Fig. 4(a), $(k_1, k_2) \in R_{II}$ in Fig. 4(b), $(k_1, k_2) \in R_{III}$ in Fig. 4(c), and $(k_1, k_2) \in R_{IV}$ in Fig. 4(d). It is quite visible that chaotic attractors have no points in Z_0 -zones (bounded by C^{E+} and C^{E-} in (a), C^{E+} and C^{M-} as well as C^{M+} and C^{E-} in (b), C^{M-} and C^{E-} in (d)).

4. Examples of bifurcation structures in (k_1, k_2) - and (b, k_2) -parameter planes

In this section we give several examples of bifurcation structures in the parameter space of map F , which are obtained numerically. In particular, Fig. 5(a) presents periodicity regions associated with attracting n -cycles, $n \leq 36$, in the (k_1, k_2) -parameter plane for $b = 0.8$, $d = 1$, $k = 0.1$, and Fig. 5(b) shows the same parameter plane with periodicity regions of n -cycles having symbolic sequence ME^{n-1} (this family of cycles is considered in detail in the next section). For $b = 0.8$ as in Fig. 5, the stability range of the actual and virtual fixed point is $-1 < k_1 < 0.9$ and $-1 < k_2 < 0.9$, respectively, so in Fig. 5 the vertical strip bounded by $k_1 = -1$ and $k_1 = 0.9$ is related to the attracting fixed point O (coexisting with other attractors for $-1 < k_2 < 0.9$), while the horizontal strip bounded by $k_2 = -1$ and $k_2 = 0.9$ is related to the attracting virtual fixed point V , and as a results, in this strip any trajectory is bounded. One more example is in Fig. 6(a), where the periodicity regions in the (b, k_2) -parameter plane are shown for $k_1 = -1.1$, $d = 1$, $k = 0.1$, and in Fig. 6(b) in the same parameter plane we present periodicity regions of n -cycles ME^{n-1} . For $k_1 = -1.1$ as in Fig. 6, the fixed point O is repelling, and the virtual fixed point V is attracting in the triangle bounded by $k_2 = -1$, $b = 1$ and $k_2 = (1 + b)/2$.

As one can see, the overall bifurcation structure of map F is quite complicated, and it is difficult to reveal all its organizing principles. However, some regularities can be recognized. For example, Fig. 7(a) shows the 1D bifurcation diagram x versus k_1 for $k_2 = 0.1$, $b = 0.8$, $d = 1$, $k = 0.1$ (the related parameter path is indicated in Fig. 5(a) by the horizontal arrow), where elements similar to those associated with a period-adding bifurcation structure can be detected, while Fig. 7(b) presents the 1D bifurcation diagram x versus k_2 for $k_1 = 1$ (along the vertical arrow in Fig. 5(a)) with elements of a period-incrementing structure with incrementing step 2. We refer to [3] for the detailed description of both structures which can be observed in the parameter space of a 1D discontinuous piecewise monotone map. Comparing Fig. 5(a) with Fig. 5(b), we can conclude that cycles ME^{n-1} are basic cycles for both these structures: see, for example, the 9-cycle $ME^8 = MUL^7$ belonging to the structure shown in Fig. 8(a) (where $k_1 = 9.5$, $k_2 = 0.1$), and coexisting 9-cycle $ME^8 = M(UL)^4$ and 11-cycle $ME^{10} = M(UL)^5$ belonging to the structure shown in Fig. 8(b) (where $k_1 = 1$, $k_2 = 0.7$). A mechanism of creation of these cycles is easy to explain: in both cases, the fixed point O is a saddle with one negative

⁷ An n -cycle $\{p_i\}_{i=0}^{n-1}$ of map F can be represented by a symbolic sequence $\sigma = \sigma_0 \dots \sigma_{n-1}$, where $\sigma_i = M$ if $p_i \in D_M$ and $\sigma_i = E$ if $p_i \in D_E$; points $p_i \in D_E$ can further be distinguished by $\sigma_i = L$ if $p_i \in D_L$ and $\sigma_i = U$ if $p_i \in D_U$.

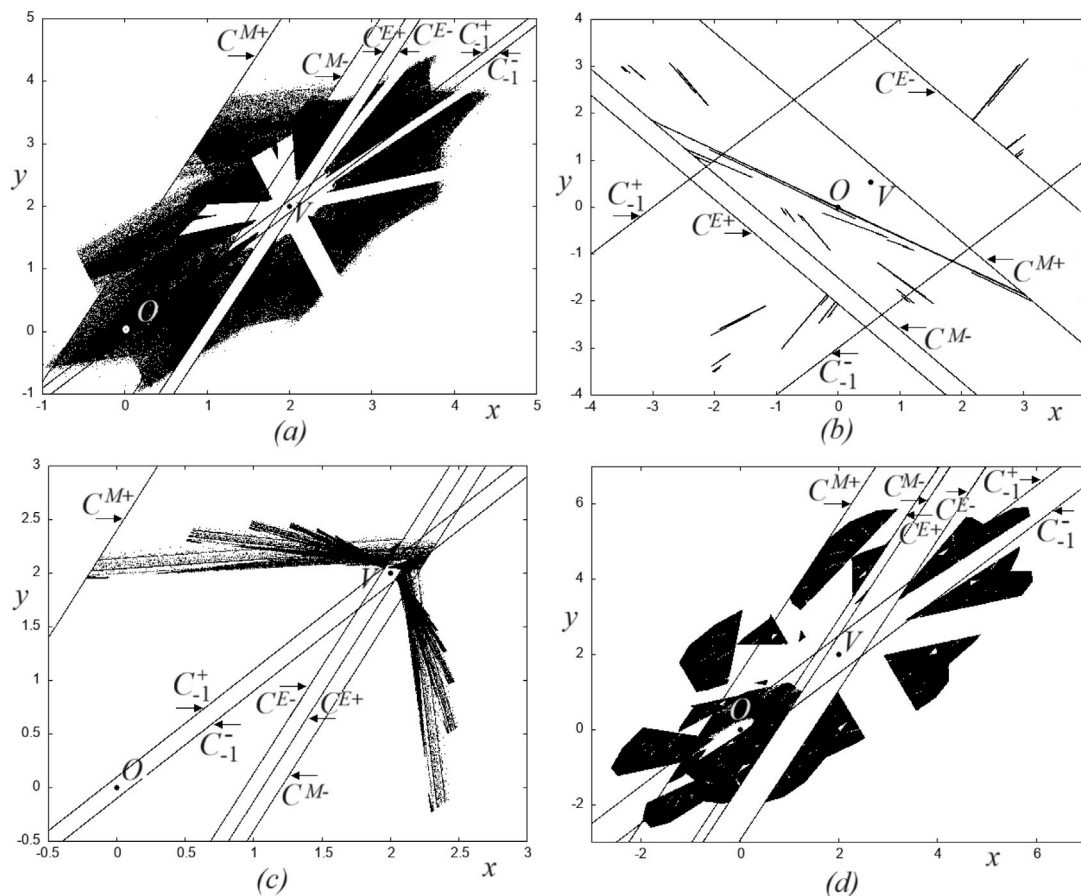


Fig. 4. Examples of chaotic attractors of map F for (a) $(k_1, k_2) \in R_I$, where $k_1 = -6, k_2 = -0.9, b = 0.5, d = 1, k = 0.1$; (b) $(k_1, k_2) \in R_{II}$, where $k_1 = -0.45, k_2 = -0.95, b = -0.9, d = 1, k = 3$; (c) $(k_1, k_2) \in R_{III}$, where $k_1 = -12, k_2 = 0.65, b = 0.5, d = 1, k = 0.1$; (d) $(k_1, k_2) \in R_{IV}$, where $k_1 = -1.5, k_2 = -0.95, b = 0.5, d = 1, k = 0.5$.

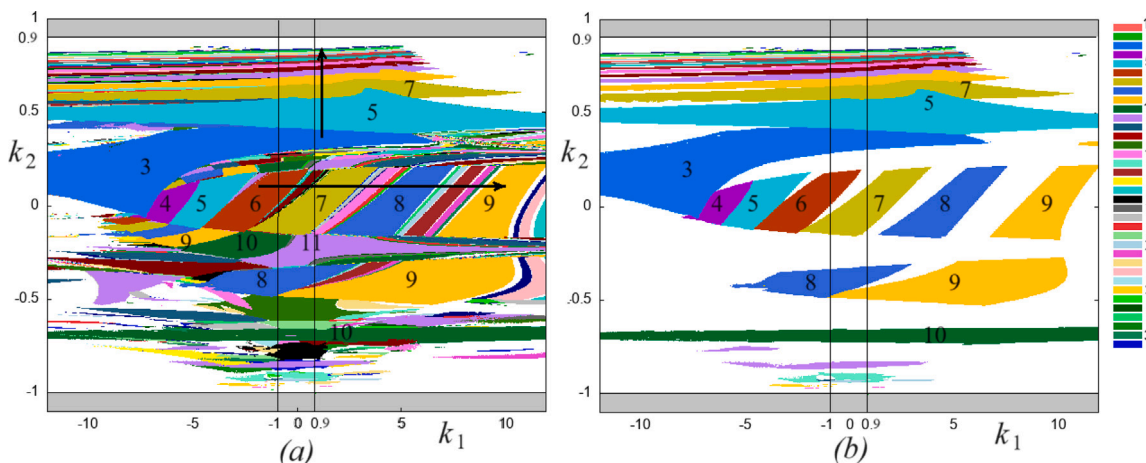


Fig. 5. (a) Periodicity regions related to attracting n -cycles, $n \leq 36$, in the (k_1, k_2) -parameter plane for $b = 0.8, d = 1, k = 0.1$. (b) The same parameter plane with periodicity regions related to attracting cycles ME^{n-1} . Here, the fixed point O is attracting in the vertical strip bounded by $k_1 = -1$ and $k_1 = 0.9$, and the virtual fixed point V is attracting in the horizontal strip bounded by $k_2 = -1$ and $k_2 = 0.9$.

and one positive eigenvalue, while the virtual fixed point V is an attracting node with one negative and one positive eigenvalue, so that starting from the leftmost periodic point, say, point $p_0 \in D_E$, the trajectory approaches V jumping from one to the other side

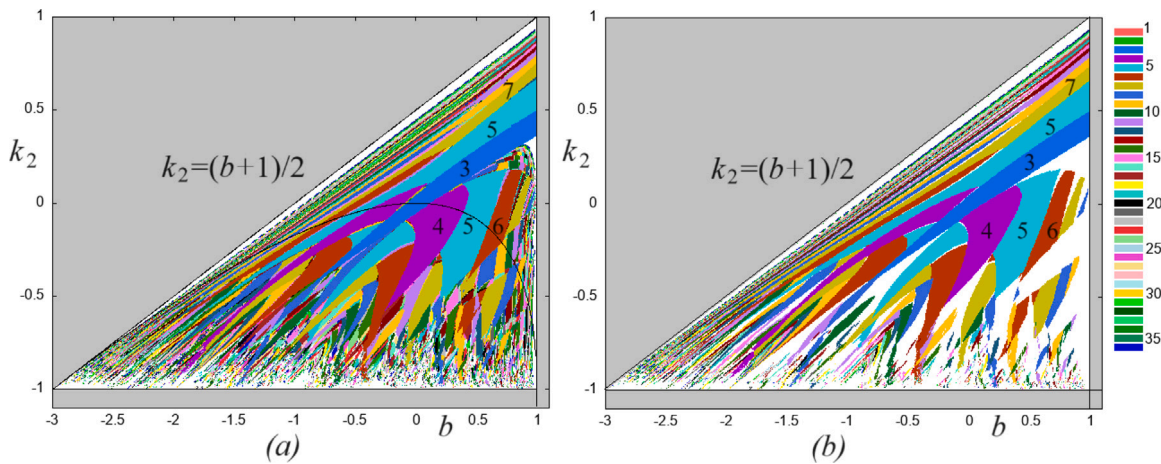


Fig. 6. (a) Periodicity regions related to attracting n -cycles, $n \leq 36$, in the (b, k_2) -parameter plane for $k_1 = -1.1$, $d = 1$, $k = 0.1$. (b) Periodicity regions related to attracting cycles ME^{n-1} . For the considered parameter values, the fixed point O is repelling and the virtual fixed point V is attracting in the triangle bounded by $k_2 = -1$, $b = 1$, $k_2 = (b + 1)/2$.

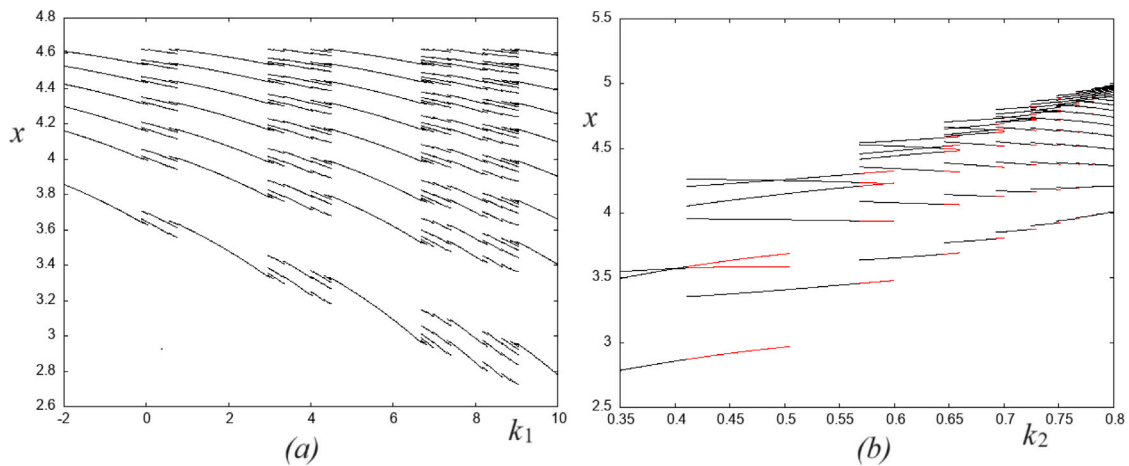


Fig. 7. 1D bifurcation diagram (a) x versus k_1 and (b) x versus k_2 for $b = 0.8$, $d = 1$, $k = 0.1$ and (a) $k_2 = 0.1$, (b) $k_1 = 1$. The related parameter paths are indicated by horizontal and vertical arrows, respectively, in Fig. 5(a). In (b), coexistence is highlighted in red. (For interpretation of the references to color in this figure legend, the reader is referred to the web version of this article.)

with respect to the eigendirection related to the positive eigenvalue of V , until it reaches the middle partition, $p_{n-1} \in D_M$, where map F_M acts sending the trajectory back to D_E : $F_M(p_{n-1}) = p_0 \in D_E$.

Before moving on to a deeper study of the cycles ME^{n-1} , we would like to stress that these multistability scenarios are particularly relevant for the potentiality of the model to replicate important stylized facts of financial markets. In fact, when two attractors characterized by quite different periodicities (like a cycle of low period and a cycle of high period or a chaotic attractor) coexist, the adding of a noise to the system may lead the dynamics of the asset price to periodically switch from a certain kind of fluctuation to another one, which is at the origin of volatility clustering of returns, fat-tails in their distribution, and so on.

5. n -cycles ME^{n-1} , $n \geq 3$

In this section we demonstrate how some family of cycles of map F can be studied, namely, how to get existence and stability conditions of a cycle belonging to a specific family. As an example, we consider the simplest family of n -cycles having symbolic sequence ME^{n-1} , $n \geq 3$, where symbol E can be substituted by L or U depending on the location of the related points of the cycle. An example is the 9-cycle $ME^8 = MUL^7$ in Fig. 8(a), or the 9- and 11-cycles $ME^8 = M(UL)^4$ and $ME^{10} = M(UL)^5$, respectively, in Fig. 8(b).

Let $p_0 = (x_0, y_0) \in D_M$ be the point of the cycle ME^{n-1} . This point satisfies the equation $F_E^{n-1} \circ F_M(x_0, y_0) = (x_0, y_0)$ which can be written as

$$J_E^{n-1}(J_M(x_0, y_0) - (x_E^*, y_E^*)) + (x_E^*, y_E^*) = (x_0, y_0)$$

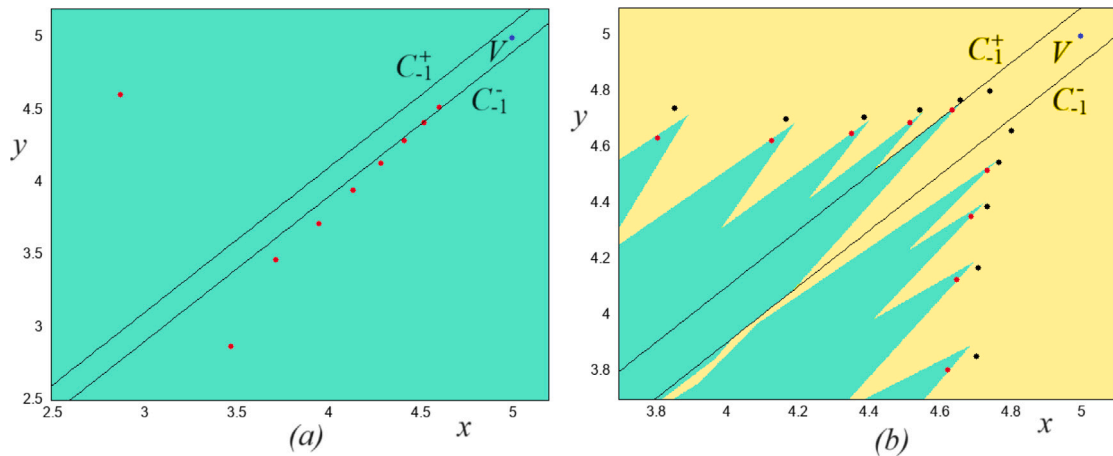


Fig. 8. (a) An attracting 9-cycle $ME^8 = MUL^7$. (b) Coexisting 11-cycle $ME^{10} = M(UL)^5$ and 9-cycles $ME^8 = M(UL)^4$ and their basins. Here $b = 0.8$, $d = 1$, $k = 0.1$ and (a) $k_1 = 9.5$, $k_2 = 0.1$, (b) $k_1 = 1$, $k_2 = 0.7$. In both cases, the fixed point O is a saddle with one negative and one positive eigenvalue.

where to simplify application of F_E^{n-1} to the point $(x_1, y_1) = F_M(x_0, y_0) = J_M(x_0, y_0)$ we make a change of variables moving the fixed point (x_E^*, y_E^*) of F_E to the origin and then, after $n - 1$ iterations, we come back to the original variables. From this equation we obtain

$$(x_0, y_0) = (J_E^{n-1} J_M - I)^{-1} (J_E^{n-1} - I)(x_E^*, y_E^*) \tag{11}$$

where $\det(J_E^{n-1} J_M - I) \neq 0$. The matrix J_E^j for any $j \geq 2$ can be represented as

$$J_E^j = \begin{pmatrix} a_j & k_2 a_{j-1} \\ a_{j-1} & k_2 a_{j-2} \end{pmatrix}$$

where a_j is a solution of the second-order linear difference equation

$$a_j = (b - k_2) a_{j-1} + k_2 a_{j-2}, \quad a_0 = 1, \quad a_1 = b - k_2 \tag{12}$$

From (11) we obtain

$$\begin{aligned} x_0 &= \frac{d}{1-b} - \frac{d}{P_{ME^{n-1}}(1)} a_{n-1} \\ y_0 &= \frac{d}{1-b} - \frac{d}{P_{ME^{n-1}}(1)} (a_{n-2} + (-k_2)^{n-1}) \end{aligned} \tag{13}$$

where $P_{ME^{n-1}}(\lambda)$ is the characteristic polynomial of the matrix $J_E^{n-1} J_M$:

$$P_{ME^{n-1}}(\lambda) = \lambda^2 - (a_{n-1}(b - k_1) + a_{n-2}(k_1 + k_2))\lambda - k_1(-k_2)^{n-1} \tag{14}$$

and it has to be $P_{ME^{n-1}}(1) \neq 0$, or, equivalently, $\det(J_E^{n-1} J_M - I) \neq 0$.

It is clear that the cycle ME^{n-1} exists only if each point of the cycle is located in its proper partition, that is, if $p_0 \in D_M$ and $p_i \in D_E$ for $1 \leq i \leq n - 1$. The existence condition $p_0 \in D_M$ leads to two inequalities, $y_0 > x_0 - k$ and $y_0 < x_0 + k$, which must be satisfied simultaneously. If $y_0 = x_0 - k$ or $y_0 = x_0 + k$, a BCB of ME^{n-1} occurs: p_0 collides with the border C_{-1}^- of D_M , or with the border C_{-1}^+ . Substituting x_0 and y_0 from (13) to $y_0 = x_0 - k$ and $y_0 = x_0 + k$, the related BCB curves denoted $BC_{0,n}^-$ and $BC_{0,n}^+$, respectively, are obtained:

$$\begin{aligned} BC_{0,n}^- : \quad & a_{n-1} - a_{n-2} - (-k_2)^{n-1} = -\frac{k}{d} P_{ME^{n-1}}(1) \\ BC_{0,n}^+ : \quad & a_{n-1} - a_{n-2} - (-k_2)^{n-1} = \frac{k}{d} P_{ME^{n-1}}(1) \end{aligned}$$

These equations can explicitly be solved with respect to k_1 :

$$\begin{aligned} BC_{0,n}^- : \quad & k_1 = \frac{1 - a_{n-1} b - a_{n-2} k_2}{a_{n-2} - a_{n-1} + (-k_2)^{n-1}} - \frac{d}{k} \\ BC_{0,n}^+ : \quad & k_1 = \frac{1 - a_{n-1} b - a_{n-2} k_2}{a_{n-2} - a_{n-1} + (-k_2)^{n-1}} + \frac{d}{k} \end{aligned}$$

Note immediately that considering some specific parameter plane, it may happen that one of these BCBs, or even both cannot occur, and thus, the related set is not involved as a boundary of the corresponding periodicity region in that plane. Moreover, only a part of each curve corresponds to a BCB of an actual cycle, namely, when all the other existence conditions are also satisfied.

The other BCB curves associated with the cycle ME^{n-1} can be obtained in a similar way. In particular, applying map F_M to the point (x_0, y_0) (see (13)) we obtain the point $p_1 = (x_1, y_1)$, where

$$\begin{aligned} x_1 &= \frac{d}{(1-b)} - \frac{d}{P_{ME^{n-1}}(1)}(1 - k_2 a_{n-2}) \\ y_1 &= \frac{d}{(1-b)} - \frac{d}{P_{ME^{n-1}}(1)} a_{n-1} \end{aligned}$$

It has to be $y_1 < x_1 - k$ or $y_1 > x_1 + k$, and from $y_1 = x_1 \mp k$, we obtain the curves $BC_{1,n}^-$ and $BC_{1,n}^+$, respectively:

$$\begin{aligned} BC_{1,n}^- : \quad & 1 - a_{n-1} - k_2 a_{n-2} = -\frac{k}{d} P_{ME^{n-1}}(1) \\ BC_{1,n}^+ : \quad & 1 - a_{n-1} - k_2 a_{n-2} = \frac{k}{d} P_{ME^{n-1}}(1) \end{aligned}$$

Then, applying to the point p_1 map F_E^{i-1} for $i = 2, \dots, n-1$, we have that all the other points of the cycle ME^{n-1} , namely, the points $p_i = (x_i, y_i)$, are as follows:

$$\begin{aligned} x_i &= \frac{d}{(1-b)} - \frac{d}{P_{ME^{n-1}}(1)}(a_{i-1}(1 - k_2 a_{n-2}) + k_2 a_{i-2} a_{n-1}) \\ y_i &= \frac{d}{(1-b)} - \frac{d}{P_{ME^{n-1}}(1)}(a_{i-2}(1 - a_n) + a_{i-1} a_{n-1}) \end{aligned} \tag{15}$$

(it is easy to check that for $i = n$ we get $(x_n, y_n) = (x_0, y_0)$), and from $y_i = x_i \mp k$, the related BCB curves are

$$\begin{aligned} BC_{i,n}^- : \quad & a_{i-1}(1 - a_{n-1} - k_2 a_{n-2}) - a_{i-2}(1 - a_n - k_2 a_{n-1}) = -\frac{k}{d} P_{ME^{n-1}}(1) \\ BC_{i,n}^+ : \quad & a_{i-1}(1 - a_{n-1} - k_2 a_{n-2}) - a_{i-2}(1 - a_n - k_2 a_{n-1}) = \frac{k}{d} P_{ME^{n-1}}(1) \end{aligned}$$

(in fact, the above equations are valid also for $i = 1$ taking into account that $a_{-1} = 0$). In particular, substituting $i = n - 1$ to (15) we have that the point $p_{n-1} = (x_{n-1}, y_{n-1})$ is defined as

$$\begin{aligned} x_{n-1} &= \frac{d}{(1-b)} - \frac{d}{P_{ME^{n-1}}(1)}(a_{n-2} + (-k_2)^{n-1}) \\ y_{n-1} &= \frac{d}{(1-b)} - \frac{d}{P_{ME^{n-1}}(1)}(a_{n-3} + (-k_2)^{n-2}(b - k_2)) \end{aligned}$$

and from $y_{n-1} = x_{n-1} \mp k$, the related BCB curves are obtained:

$$\begin{aligned} BC_{n-1,n}^- : \quad & a_{n-2} - a_{n-3} - b(-k_2)^{n-2} = -\frac{k}{d} P_{ME^{n-1}}(1) \\ BC_{n-1,n}^+ : \quad & a_{n-2} - a_{n-3} - b(-k_2)^{n-2} = \frac{k}{d} P_{ME^{n-1}}(1) \end{aligned}$$

Since we consider periodicity regions related to attracting cycles, these regions can be bounded, besides the BCB curves, by the curves associated with the loss of stability of the cycles. For the cycle ME^{n-1} , let us suppose that it has no points belonging to the discontinuity lines (i.e., ME^{n-1} does not undergo a BCB) and thus its eigenvalues, say $\lambda_{1,n}$ and $\lambda_{2,n}$, are well defined. The stability conditions for ME^{n-1} are $\{P_{ME^{n-1}}(1) > 0, P_{ME^{n-1}}(-1) > 0, \det J_E^{n-1} J_M < 1\}$, where $P_{ME^{n-1}}(\lambda)$ is defined in (14). Given that both maps, F_M and F_E , are linear, an attracting cycle ME^{n-1} can lose stability only via degenerate bifurcations: the conditions $\lambda_{1,n} = 1$ and $\lambda_{2,n} = -1$ are associated with degenerate transcritical and degenerate flip bifurcations, respectively, and complex-conjugate eigenvalues on the unit circle are related to a center bifurcation. The corresponding bifurcation curves denoted P_n^1, P_n^{-1} and C_n , respectively, can be obtained from $P_{ME^{n-1}}(1) = 0, P_{ME^{n-1}}(-1) = 0$ and $\det J_E^{n-1} J_M = 1$:

$$\begin{aligned} P_n^1 : \quad & 1 - a_{n-1}(b - k_1) - a_{n-2}(k_1 + k_2) - k_1(-k_2)^{n-1} = 0 \\ P_n^{-1} : \quad & 1 + a_{n-1}(b - k_1) + a_{n-2}(k_1 + k_2) - k_1(-k_2)^{n-1} = 0 \\ C_n : \quad & -k_1(-k_2)^{n-1} = 1 \end{aligned}$$

Clearly, these curves are only valid for an actual cycle for which all the existence conditions are satisfied.

Note that all the equations of the BCB and stability curves obtained above can be solved with respect to k_1 .

To summarize, we can state the following

Proposition. Map F in (8) has an attracting n -cycle ME^{n-1} , $n \geq 3$, if the following inequalities are satisfied:

$$\left\{ \begin{aligned} & P_{ME^{n-1}}(1) > 0, \quad P_{ME^{n-1}}(-1) > 0, \quad -k_1(-k_2)^{n-1} < 1, \\ & -k P_{ME^{n-1}}(1)/d < a_{n-1} - a_{n-2} - (-k_2)^{n-1} < k P_{ME^{n-1}}(1)/d, \\ & \text{and for } i = 1, \dots, n-1, \\ & a_{i-1}(1 - a_{n-1} - k_2 a_{n-2}) - a_{i-2}(1 - a_n - k_2 a_{n-1}) < -k P_{ME^{n-1}}(1)/d \text{ or} \\ & a_{i-1}(1 - a_{n-1} - k_2 a_{n-2}) - a_{i-2}(1 - a_n - k_2 a_{n-1}) > k P_{ME^{n-1}}(1)/d \end{aligned} \right.$$

where a_j is a solution of the second-order linear difference equation given in (12), and $P_{ME^{n-1}}(\lambda)$ is defined in (14).

As an example, in Fig. 9(a) we show the periodicity region associated with the attracting cycle ME^2 , whose boundaries are plotted using the equations given above, in the (k_1, k_2) -parameter plane for the other parameter values as in Fig. 5(a). As one can see, in Fig. 9(a) the 3-periodicity region is bounded by proper arcs of the BCB curves $BC_{0,3}^+, BC_{0,3}^-, BC_{2,3}^-$, and the stability curves P_3^{-1} (related to a degenerate flip bifurcation of the cycle ME^2) and C_3 (related to a center bifurcation of ME^2), while in Fig. 9(b),

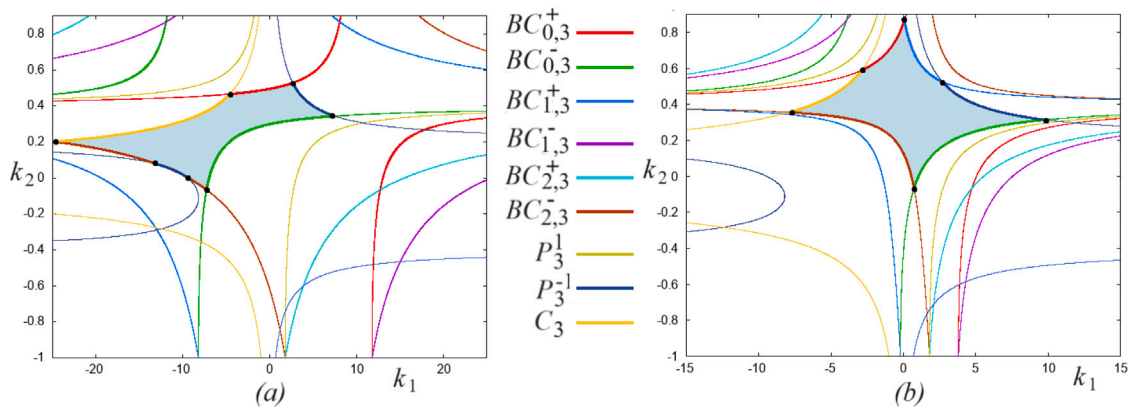


Fig. 9. Boundaries of the 3-periodicity region (shown in light blue) related to an attracting cycle ME^2 in the (k_1, k_2) -parameter plane for $b = 0.8, d = 1$ and (a) $k = 0.1$, (b) $k = 0.5$. Codimension-two bifurcation points of the cycle ME^2 are marked by black circles. (For interpretation of the references to color in this figure legend, the reader is referred to the web version of this article.)

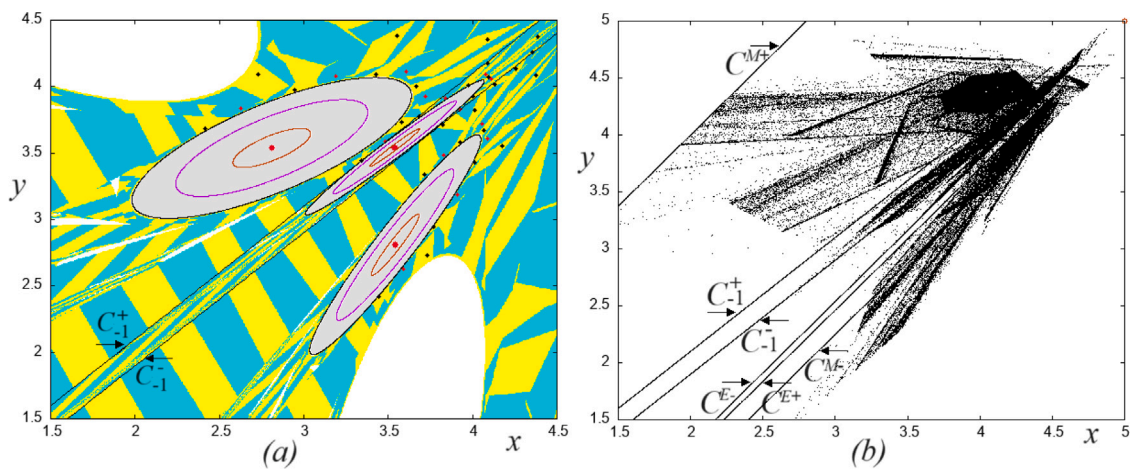


Fig. 10. (a) Cyclic F^3 -invariant regions (shown in gray with white preimages) bounded by ellipses with centers at points of the cycle ME^2 undergoing a center bifurcation, and coexisting attracting 14- and 29-period cycles (with blue and yellow basins). (b) Chaotic attractor of map F . Here $b = 0.8, d = 1, k = 0.1$ and (a) $k_1 = -6.15, k_2 = \sqrt{-1/k_1}$, (b) $k_1 = -12, k_2 = 0.3$. (For interpretation of the references to color in this figure legend, the reader is referred to the web version of this article.)

where $k = 0.5$ (and all the other parameter values are as before), also an arc of the BCB curve $BC_{1,3}^+$ bounds the 3-periodicity region. Note that in Fig. 9 all the BCB and stability curves associated with cycle ME^2 are plotted to also show those curves which, in the considered case, are not involved as the boundaries of the 3-periodicity region in the (k_1, k_2) -parameter plane (e.g., the curves $BC_{1,3}^-$ and $BC_{2,3}^+$).

The center bifurcation of 3-cycle ME^2 is illustrated in Fig. 10(a), where $k_1 = -6.15, k_2 = \sqrt{-1/k_1}$ and other parameters are as in Fig. 5. In this case, three cyclic F^3 -invariant regions (filled by quasiperiodic trajectories and bounded by ellipses with centers at the points of the cycle ME^2) coexist with attracting 14- and 29-cycles. An example of a chaotic attractor which can appear after a center bifurcation, is shown in Fig. 10(b) where the former F^3 -invariant regions (having higher density) are still visible.

Let us apply now the results presented in this section to the family of cycles $ME^{n-1}, n \geq 3$. Considering again the periodicity regions shown in Fig. 5(b) and Fig. 6(b) which are obtained numerically, we now plot their boundaries using the analytical expressions of these boundaries taking into account all the existence and stability conditions of the related cycles: to compare, in Fig. 11(a) and Fig. 11(b) these boundaries are superimposed on the periodicity regions shown in Fig. 5(b) and Fig. 6(b), respectively.

To give more details, in Fig. 12(a) the BCB and stability boundaries of the periodicity regions associated with attracting cycles $ME^{n-1}, n = 3, \dots, 36$, are plotted in different colors in the (k_1, k_2) -parameter plane for the other parameter values fixed as in Fig. 5. It is interesting to see two partially overlapping substructures which are better visible in Fig. 12(b) presenting magnified window indicated in Fig. 12(a) by black rectangle. One can check that one substructure (with lower and upper boundaries defined by decreasing functions) is related to even-period cycles, while the second substructure (with lower and upper boundaries defined by increasing functions) is related to odd-period cycles (the 1D bifurcation diagram in Fig. 7(b) is a cross-section of this substructure

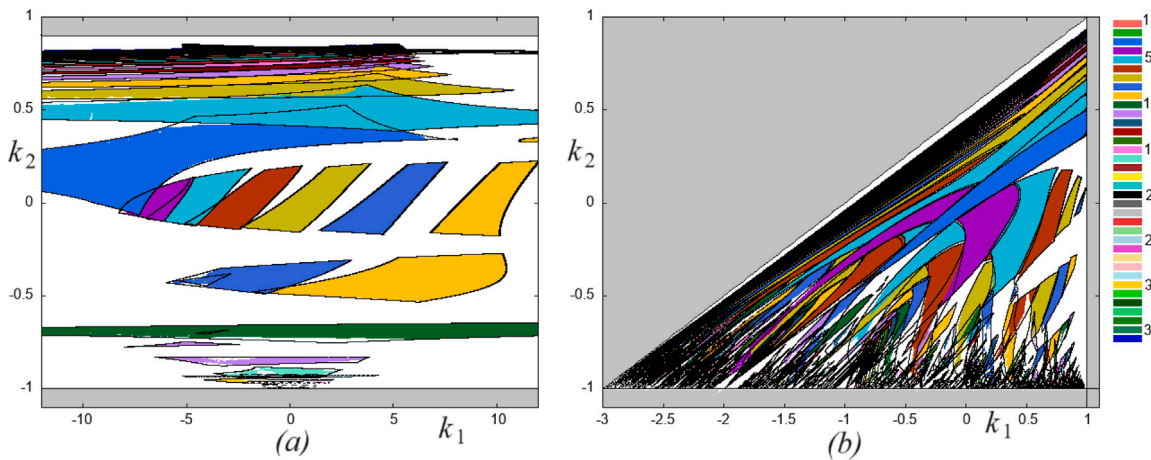


Fig. 11. BCB and stability boundaries of the periodicity regions related to the attracting cycles ME^{n-1} , $n = 3, \dots, 36$, plotted (in black) using their analytical expressions, which are superimposed on the periodicity regions obtained numerically: (a) to compare with Fig. 5(b), and (b) to compare with Fig. 6(b).

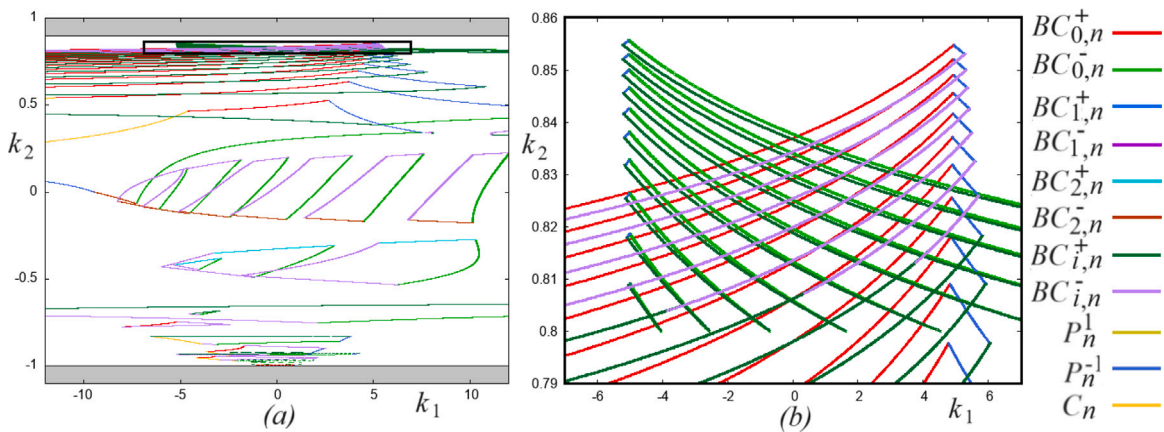


Fig. 12. (a) BCB and stability boundaries of the periodicity regions related to attracting cycles ME^{n-1} , $n = 3, \dots, 36$, in the (k_1, k_2) -parameter plane for $b = 0.8$, $d = 1$, $k = 0.1$. (b) Magnification of the black rectangle indicated in (a). Overlapping parts of the periodicity regions correspond to multistability.

for lower values of k_2 , namely, for $0.35 < k_2 < 0.8$, $k_1 = 1$, see the vertical arrow in Fig. 5(a). The same two substructures in the (b, k_2) -parameter plane can be seen in the inset in Fig. 13(a) which shows magnified window indicated by the black rectangle. In Fig. 13, the BCB and stability boundaries of the periodicity regions related to the cycles ME^{n-1} , $n = 3, \dots, 36$, are plotted in the (b, k_2) -parameter plane for the other parameter values fixed as in Fig. 6. Fig. 13(b) shows magnified window indicated in Fig. 13(a) by red rectangle, where one can better see some substructures “issuing” from the points $(b, k_2) = (b_{m/n}, -1)$, $b_{m/n} = 2 \cos(2\pi m/n) - 1$, associated with $\det J_E = 1$ and rational rotation numbers m/n of the matrix J_E , e.g., from the points $(b, k_2) = (b_{1/3}, -1) = (-2, -1)$, $(b, k_2) = (b_{1/4}, -1) = (-1, -1)$, $(b, k_2) = (b_{1/5}, -1) = ((\sqrt{5}-3)/2, -1)$, etc. The inset in Fig. 13(b) shows magnified substructure “issuing” from the point $(b, k_2) = (-1, -1)$ associated with rotation number $1/4$. More detailed investigation of these and other substructures is left for future studies.

6. Conclusions

The presence of periodic and chaotic dynamics, together with the scenarios of multistability are of extreme relevance for the possibility of replicating important stylized facts of financial markets. Chaotic motion causes the unpredictability typical of asset prices and the alternation of bubbles and crashes. Even more interestingly can be the scenarios where different attractors coexist. In particular, when an attractor characterized by low variability of the dynamics (periodic of low period, or even a stable equilibrium) coexists with another stable attractor causing price fluctuations of large amplitude (periodic of high period or chaotic attractor), this can be the perfect basis to replicate some other stylized facts of financial markets, such as volatility clustering, simply by introducing some stochastic element into the model. In our future works we plan to deepen the consequences for the financial market of the results obtained in the present paper. We would like, not only to introduce some noise into the picture, but also to

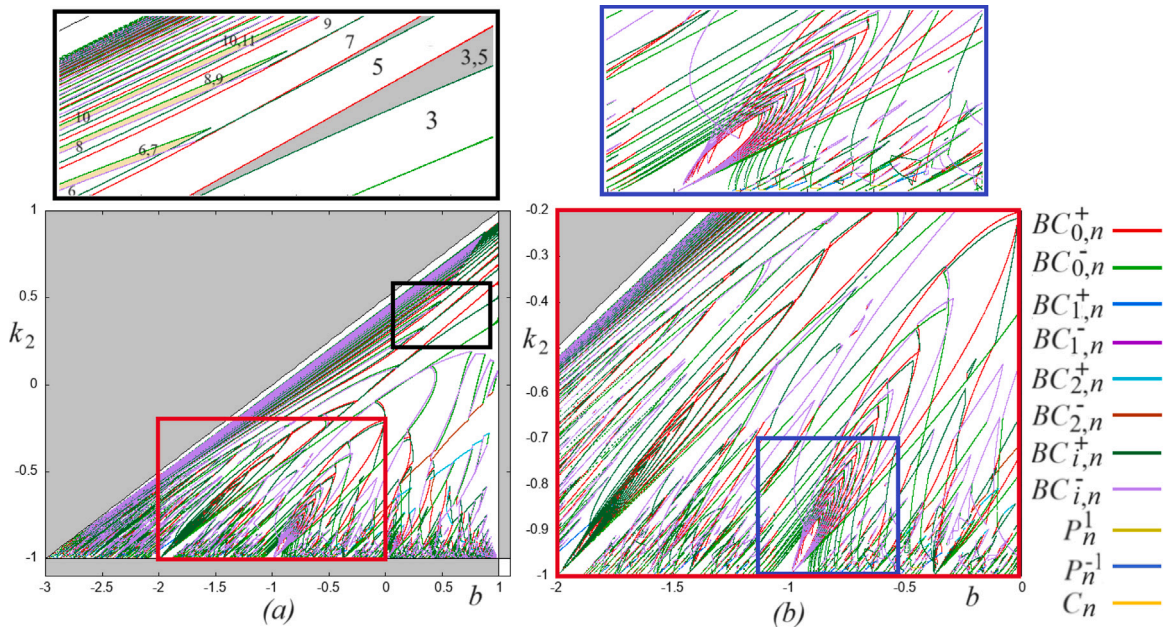


Fig. 13. (a) BCB and stability boundaries of the periodicity regions related to attracting cycles ME^{n-1} , $n = 3, \dots, 36$, in the (b, k_2) -parameter plane for $k_1 = -1.1$, $d = 1$, $k = 0.1$. The inset shows the magnified black rectangle. (b) Magnification of the red rectangle indicated in (a); the inset shows the magnified blue rectangle. (For interpretation of the references to color in this figure legend, the reader is referred to the web version of this article.)

consider other kinds of traders, the possibility for traders to switch from one strategy to another one, and more price trend thresholds (i.e. more regimes). From a dynamical point of view, specific properties of the two-dimensional piecewise-linear discontinuous map described in the present paper lead to quite complex bifurcation structure of the parameter space. We obtained the boundaries of the periodicity regions associated with attracting cycles having one point in the middle partition and all other points outside it. These cycles are basic to structures with some elements of period-adding and period-incrementing bifurcation structures (well described for one-dimensional discontinuous piecewise monotone maps), which are worth describing in more detail, as well as bifurcation structures related to other cycles and chaotic attractors.

Declaration of competing interest

The authors declare that they have no known competing financial interests or personal relationships that could have appeared to influence the work reported in this paper.

Acknowledgments

Iryna Sushko acknowledges the partial financial support of the NAS of Ukraine within the scope of the project “Mathematical modeling of complex dynamical systems and processes caused by the state security” (grant number 0123U100853), as well as by the UC Berkeley Economics/Haas and the Universities for Ukraine Non-Residential Fellowship program. She is also grateful to the University of Urbino, DESP, for the hospitality during her stay there as a visiting researcher.

The work of Fabio Tramontana has been funded by the PRIN 2022 under the Italian Ministry of University and Research (MUR) Prot. 2022YMLS4T - TEC - Tax Evasion and Corruption: theoretical models and empirical studies. A quantitative-based approach for the Italian case.

References

- [1] M. Anufriev, L. Gardini, D. Radi, Chaos, border collisions and stylized empirical facts in an asset pricing model with heterogeneous agents, *Nonlinear Dynam.* 102 (2020) 993–1017.
- [2] V. Avrutin, A. Dal Forno, U. Merlone, Codimension-2 bifurcations in a quantum decision making model, *J. Bifurcation Chaos* 33 (13) (2023) 2330032.
- [3] V. Avrutin, L. Gardini, I. Sushko, F. Tramontana, *Continuous and Discontinuous Piecewise-Smooth One-Dimensional Maps: Invariant Sets and Bifurcation Structures*, World Scientific, Singapore, 2019.
- [4] G. Campisi, A. Panchuk, F. Tramontana, A discontinuous model of exchange rate dynamics with sentiment traders, *Ann. Oper. Res.* (2023) <http://dx.doi.org/10.1007/s10479-023-05387-2>.
- [5] R. Cont, Empirical properties of asset returns: stylized facts and statistical issues, *Quant. Finance* 1 (2) (2001) 223–236.
- [6] R.H. Day, W. Huang, Bulls, bears and market sheep, *J. Econ. Behav. Organ.* 14 (3) (1990) 299–329.

- [7] M. di Bernardo, C.J. Budd, A.R. Champneys, P. Kowalczyk, Piecewise-Smooth Dynamical Systems: Theory and Applications, in: Appl. Math. Sci., vol. 163, Springer, New York, 2008.
- [8] L. Gardini, D. Radi, N. Schmitt, I. Sushko, F. Westerhoff, Causes of fragile stock market stability, *J. Econ. Behav. Organ.* 200 (2022) 483–498.
- [9] L. Gardini, D. Radi, N. Schmitt, I. Sushko, F. Westerhoff, Perception of fundamental values and financial market dynamics: Mathematical insights from a 2D piecewise-linear map, *SIAM J. Appl. Dyn. Syst.* 21 (2022) 2314–2337.
- [10] L. Gardini, D. Radi, N. Schmitt, I. Sushko, F. Westerhoff, A 2D piecewise-linear discontinuous map arising in stock market modeling: Two overlapping period-adding bifurcation structures, *Chaos Solitons Fractals* 176 (2023) 114143.
- [11] W. Huang, R. Day, Chaotically switching bear and bull markets: the derivation of stock price distributions from behavioral rules, in: R. Day, P. Chen (Eds.), *Nonlinear Dynamics and Evolutionary Economics*, Oxford University Press, Oxford, 1993, pp. 169–182.
- [12] W. Huang, H. Zheng, Financial crisis and regime-dependent dynamics, *J. Econ. Behav. Organ.* 82 (2012) 445–461.
- [13] W. Huang, H. Zheng, H. Chia, Financial crisis and interacting heterogeneous agents, *J. Econom. Dynam. Control* 34 (2010) 1105–1122.
- [14] T. Lux, M. Ausloos, The science of disasters, in: *Market Fluctuations I: Scaling, Multiscaling, and Their Possible Origins*, Springer, New York, 2002, pp. 372–409.
- [15] T. Lux, M. Marchesi, Scaling and criticality in a stochastic multi-agent model of a financial market, *Nature* 397 (1999) 498–500.
- [16] S. Manzan, F. Westerhoff, Heterogeneous expectations, exchange rate dynamics and predictability, *J. Econ. Behav. Organ.* 64 (2007) 111–128.
- [17] C. Mira, Embedding of a Dim1 piecewise continuous and linear leonov map into a Dim2 invertible map, in: *Global Analysis of Dynamic Models for Economics, Finance and Social Sciences*, Springer, New York, 2013, pp. 337–368.
- [18] C. Mira, L. Gardini, A. Barugola, J.C. Cathala, *Chaotic Dynamics in Two-Dimensional Noninvertible Maps*, World Scientific, Singapore, 1996.
- [19] H.E. Nusse, J.A. Yorke, Border-collision bifurcations including ‘period two to period three’ bifurcation for piecewise smooth systems, *Physica D* 57 (1992) 39–57.
- [20] H.E. Nusse, J.A. Yorke, Border-collision bifurcations for piecewise smooth one dimensional maps, *Int. J. Bifurcation Chaos* 5 (1995) 189–207.
- [21] B. Rakshit, M. Apratim, S. Banerjee, Bifurcation phenomena in two-dimensional piecewise smooth discontinuous maps, *Chaos* 20 (2010) 033101.
- [22] D. Simpson, *Bifurcations in Piecewise-Smooth Continuous Systems*, in: *World Scientific Series on Nonlinear Science*, vol. 70, World Scientific, Singapore, 2010.
- [23] D. Simpson, Unfolding codimension-two subsumed homoclinic connections in two-dimensional piecewise-linear maps, *Int. J. Bifurcation Chaos* 30 (3) (2020) 2030006.
- [24] I. Sushko, L. Gardini, Center bifurcation for two-dimensional border-collision normal form, *Int. J. Bifurcation Chaos* 18 (2008) 1029–1050.
- [25] I. Sushko, L. Gardini, Degenerate bifurcations and border collisions in piecewise smooth 1D and 2D maps, *Int. J. Bifurcation Chaos* 20 (2010) 2045–2070.
- [26] I. Sushko, L. Gardini, K. Matsuyama, Dynamics of a generalized fashion cycle model, *Chaos Solitons Fractals* 126 (2019) 135–147.
- [27] F. Tramontana, F. Westerhoff, L. Gardini, On the complicated price dynamics of a simple one-dimensional discontinuous financial market model with heterogeneous interacting traders, *J. Econ. Behav. Org.* 74 (2010) 187–205.
- [28] F. Tramontana, F. Westerhoff, L. Gardini, The bull and bear market model of Huang and day: Some extensions and new results, *J. Econom. Dynam. Control* 37 (2013) 2351–2370.
- [29] F. Tramontana, F. Westerhoff, L. Gardini, One-dimensional maps with two discontinuity points and three linear branches: mathematical lessons for understanding the dynamics of financial markets, *Dec. Econ. Fin.* 37 (2014) 27–51.
- [30] Zh. T. Zhusubaliyev, E. Mosekilde, *Bifurcations and Chaos in Piecewise-Smooth Dynamical Systems*, in: *World Sci. Ser. Nonlinear Sci. Ser. A Monogr. Treatises*, vol. 44, World Scientific, Hackensack, NJ, 2003.